Article

Migration of human T cells can be differentially directed by electric fields depending on the extracellular microenvironment

Electrotaxis of CD4+ and CD8+ T cells

Karen Ende,
Fabião Santos,
Judith Guasch, Ralf
Kemkemer

ralf.kemkemer@
reutlingen-university.de

Highlights

Human CD4+ and CD8+ T cells show anodal electrotaxis on 2D substrates

Human T cell electrotaxis depends on T cell type and substrate coating

T cell electrotaxis differs in 2D and 3D environment

The effect of EFs on T cell differentiation and apoptosis is not significant

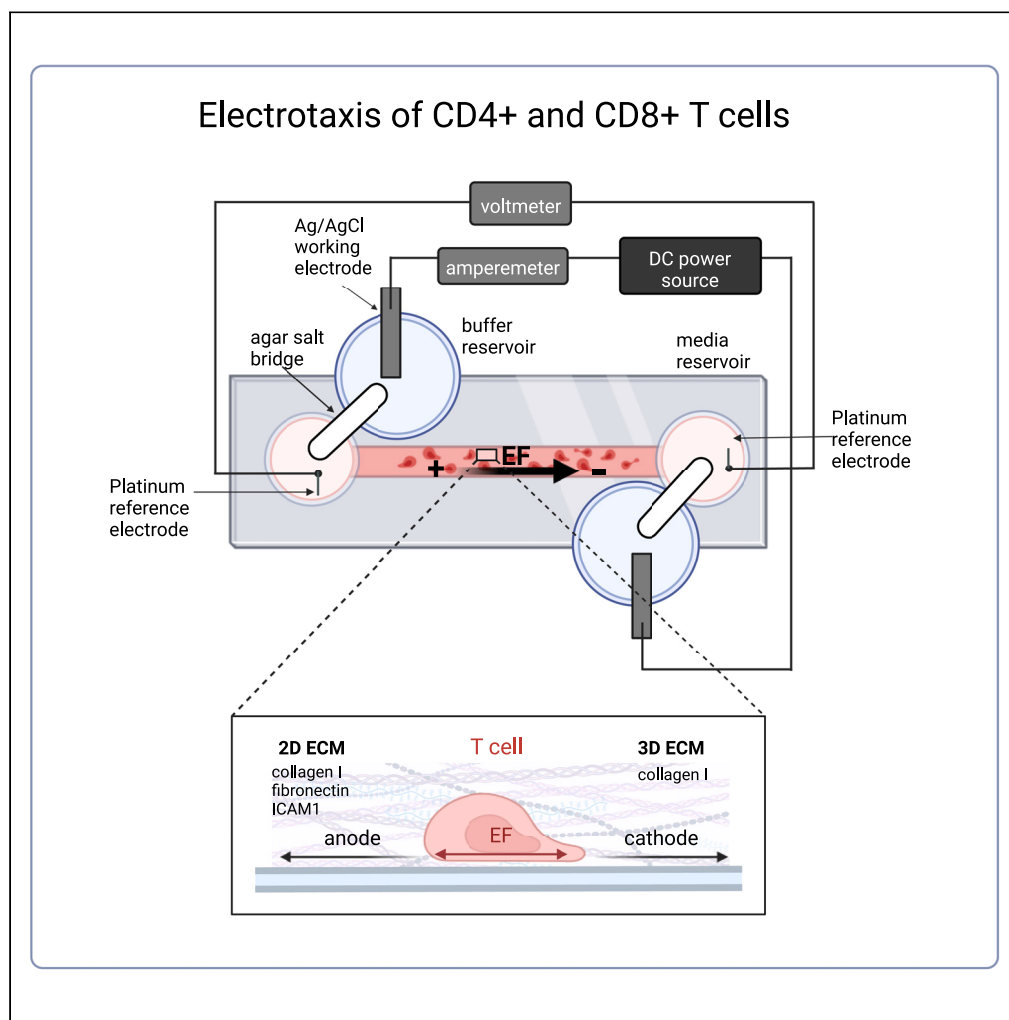## Article

Migration of human T cells can be differentially directed by electric fields depending on the extracellular microenvironment

Karen Ende,[1] Fabião Santos,[2,3,4] Judith Guasch,[2,3,4] and Ralf Kemkemer[1,5,6,*]

SUMMARY

T cell migration plays an essential role in the immune response and T cell-based therapies. It can be modulated by chemical and physical cues such as electric fields (EFs). The mechanisms underlying electrotaxis (cell migration manipulated by EFs) are not fully understood and systematic studies with immune cells are rare. In this *in vitro* study, we show that direct current EFs with strengths of physiologically occurring EFs (25–200 mV/mm) can guide the migration of primary human CD4$^+$ and CD8$^+$ T cells on 2D substrates toward the anode and in a 3D environment differentially (CD4$^+$ T cells show cathodal and CD8$^+$ T cells show anodal electrotaxis). Overall, we find that EFs present a potent stimulus to direct T cell migration in different microenvironments in a cell-type-, substrate-, and voltage-dependent manner, while not significantly influencing T cell differentiation or viability.

INTRODUCTION

Cell migration plays a crucial role in various physiological and pathophysiological processes, such as wound healing, cancer, and the immune response.[1] Specifically, immune cells can switch between different migration modes (in 2D a mainly adhesion-dependent "mesenchymal" and in 3D an adhesion-independent "ameboid" migration mode), as they are required to migrate efficiently and autonomously in various environments of different chemical and physical compositions (e.g., within lymph nodes, blood vessel walls, peripheral tissue, tumors, etc.) to fulfill biological functions in an immune response.[2–10]

Cell migration appears random when no directed external stimulus is applied, but can be manipulated and directed by external cues, such as chemical gradients (chemotaxis), topography (topotaxis), substrate stiffness (durotaxis), surface-bound ligands (haptotaxis), temperature (thermotaxis), and electric fields (electrotaxis or galvanotaxis).[3,7,11–13] Electrotaxis has been minimally assessed in the context of T cells and specifically in 3D environments; furthermore, the underlying general cellular mechanisms of electrotaxis remain to be fully elucidated.

Endogenous EFs appear in many physiological and pathophysiological processes such as wound healing, embryonic development, tumor growth, and regeneration.[14–17] For example, when an epithelial layer is disrupted, an EF is generated by ion flux, leading to transepithelial potential differences at the wound site, resulting in EF voltages of 15–200 mV/mm near the wound.[18] Furthermore, EFs of similar strength could be detected on the tumor surface of murine tumor allografts.[17]

EFs can direct the cell migration of various cell types and can even override biochemical and topographical signals.[13,19,20] Moreover, it has been shown that the effects of EFs are cell-type specific, and even cells from the same lineage can show different migration directionality in EFs.[21,22] Next to EFs, the extracellular microenvironment affects cell migration and can also alter the directionality of cells in an EF, especially when comparing 2D vs. 3D environments.[23] Additionally, EFs have the ability to affect various cell functions, including activation, proliferation, and differentiation.[22,24,25] Only a few studies have focused on immune cells[22,26] or specifically, on T cell electrotaxis,[20,25,27,28] even though electrotaxis might be promising for conditions where T cell functions are dysregulated such as the tumor microenvironment. T cells can be mainly divided into two types, which are important in mounting immunological responses toward cancer[29,30] as well as inflammatory and autoimmune diseases.[31,32] In general terms, CD4$^+$ T cells, known as helper T cells, direct the immune response by activating effector T cells. CD8$^+$ T cells, known as cytotoxic T cells, can recognize and destroy cancer cells.

Electric fields might offer future potential for *in vivo* applications in T cell-based therapies. Despite the great success of T cell therapies for hematological cancers,[33] the effectiveness of such immunotherapies for solid tumors is dependent on the successful tumor infiltration of engineered T cells.[34–36] EFs might offer the possibility to improve T cell infiltration, by guiding T cells efficiently into the tumor and might be specifically useful against "cold" tumors. Cold tumors have an immunosuppressive microenvironment including a high-density ECM that

[1]Reutlingen Research Institute and School of Life Sciences, Reutlingen University, 72762 Reutlingen, Germany
[2]Institute of Materials Science of Barcelona (ICMAB-CSIC), Campus UAB, 08193 Bellaterra, Spain
[3]Dynamic Biomimetics for Cancer Immunotherapy, Max Planck Partner Group, ICMAB-CSIC, Campus UAB, 08193 Bellaterra, Spain
[4]Centro de Investigación Biomédica en Red de Bioingeniería, Biomateriales y Nanomedicina (CIBER-BBN), 28029 Madrid, Spain
[5]Department of Cellular Biophysics, Max Planck Institute for Medical Research, 69120 Heidelberg, Germany
[6]Lead contact
*Correspondence: ralf.kemkemer@reutlingen-university.de
https://doi.org/10.1016/j.isci.2024.109746

needs to be overcome by T cells in order to infiltrate and fight the tumor.[37] Furthermore, it was found that tumors themselves generate endogenous small EFs on the tumor surface (measured *ex vivo*).[17] Thus, it is important to elucidate the impact of tumor EFs on T cells, specifically on engineered or cytotoxic T cells to improve T cell-based tumor therapies.

Since directed migration is a key functionality of T cells in physiological and pathophysiological processes, we investigated the migration of primary human CD4+ and CD8+ T cells, and their ability to respond to EF exposure, at various physiologically relevant EF strengths, ranging from 25 to 200 mV/mm. We further evaluated how the extracellular microenvironment is affecting T cell electrotaxis. More specifically, CD4+ and CD8+ T cell electrotaxis was experimentally assessed on various 2D substrate coatings, namely human fibronectin (FN), human intercellular adhesion molecule 1 (ICAM1), and bovine collagen type I (collagen), and additionally in 3D collagen gels. Moreover, we investigated the influence of EFs on T cell functionality and analyzed cell viability, apoptosis, and the differentiation of different T cell subtypes.

RESULTS

The influence of physiological strength direct current (dc) EFs on T cell migration was investigated, and the electrotactic response was found to be dependent on cell type, voltage, and substrate coating. However, previous studies, have reported that human T cells migrate toward the cathode when exposed to dc EFs.[25,27,28] While, in this case, the results show a significantly directed migration toward the anode (except for CD4+ T cells in 3D collagen gels showing cathodal electrotaxis) when primary human CD4+ and CD8+ T cells are exposed to dc EF strengths between 25 and 200 mV/mm on different 2D substrates and in 3D environments.

Cells were observed with time-lapse video microscopy, and cell movement was tracked for three conditions: without EF stimulus (noEF), applied EF stimulus (EF), and after reversal of EF polarity (EFrev). Representative images and migration tracks of CD8+ T cells on three substrate coatings at an EF strength of 100 mV/mm are shown in Figure 1 (see Figure S1 for representative images and migration tracks at different EF strengths revealing a voltage-dependent directed migration of CD8+ T cells). The cell migration tracks in Figure 1 reveal a random migration of CD8+ T cells without EF application. A directed migration toward the anode (left) can be observed when an EF of 100 mV/mm was applied. The migration direction is changed to the "new anode" (right) after the EF polarity was reversed. Depending on the substrate coating, different characteristics of the electrotactic migration can be observed.

T cells show anodal electrotaxis on fibronectin and ICAM1-coated substrates and migration directionality increases with increasing electric field strength

On FN- and ICAM1-coated substrates, primary human CD4+ (Figure 2A) and CD8+ (Figure 2B) T cells show electrotaxis toward the anode. The cell migration tracks in Figures 2A and 2B reveal a directed migration toward the anode (left) and a changed direction to the "new anode" (right) after the EF was reversed.
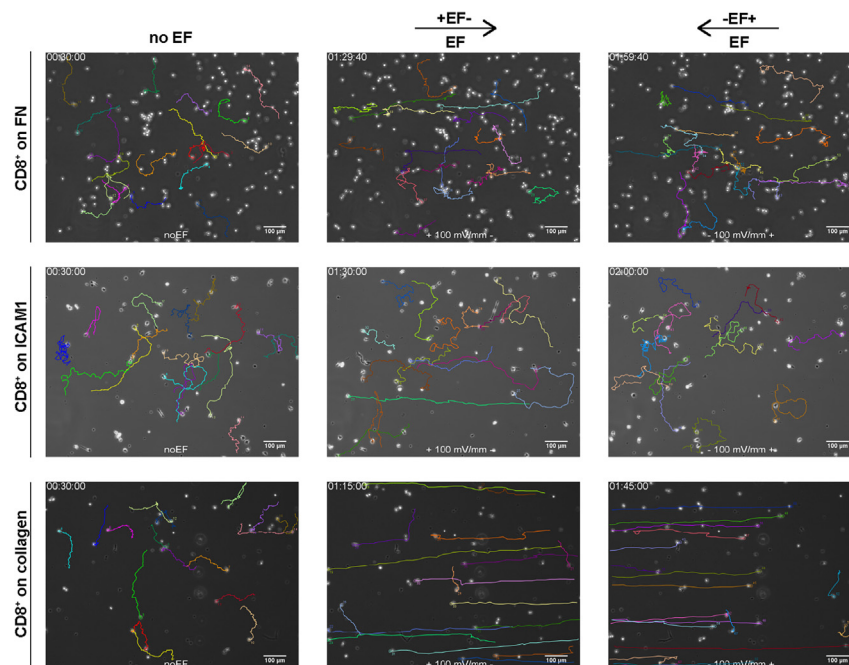
Figure 1. Representative phase-contrast images of CD8+ T cells migrating on differently coated substrates
FN, ICAM1, or collagen at 100 mV/mm. Cells were manually tracked for 30 min (colored lines), without stimulation (noEF), during EF exposure (EF) (anode (+) on the left, cathode (−) on the right), after 30 min the EF direction was reversed (EF rev) (EF polarity was changed: anode (+) on the right, cathode (−) on the left). On collagen-coated substrate (lower row) cells were tracked for shorter time periods (15 min), due to fast directed T cell migration. Scale bar: 100 μm.
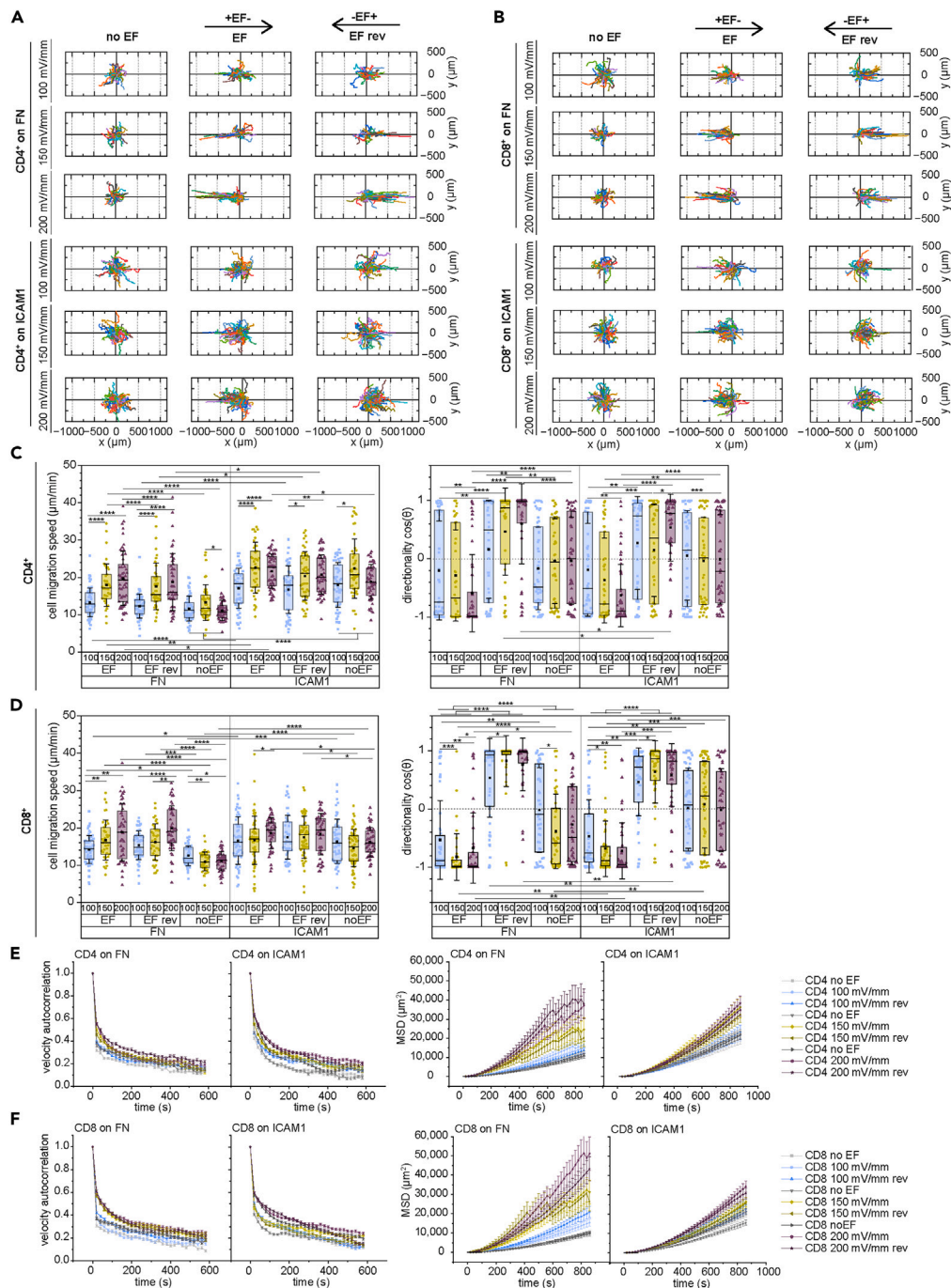
Figure 2. CD4^{+} and CD8^{+} T cells migrate toward the anode on FN- and ICAM1-coated substrates

Migration directionality and speed are dependent on T cell type, substrate coating, and EF strength. Migration of CD4^{+} and CD8^{+} T cells on FN- or ICAM1-coated substrates, stimulated with 3 different EF strengths (100, 150, and 200 mV/mm), and without stimulation (noEF) was studied. The EF was applied for a total of 60 min: 30 min with EF and 30 min with reversed EF direction (EF rev) (EF polarity was changed) (frame rate 10 s). Migration tracks of CD4^{+} (A) and CD8^{+} (B) T cells on FN- or ICAM1-coated substrates and at 3 different EF strengths, without stimulation (no EF), EF stimulation (EF), and after EF reversal (EF rev), over the 30 min time-period respectively. Boxplots of cell migration speed and migration directionality of CD4^{+} (C) and CD8^{+} (D) T cells (error bars are SD). Velocity autocorrelation and mean squared displacement (error bars are SEM) of CD4^{+} (E) and CD8^{+} (F) T cells. Statistical significance was determined with Mann-Whitney Test (*$p < 0.05$, **$p < 0.01$, ***$p < 0.001$, ****$p < 0.0001$). For all: min. 3 independent experiments ($N_{donors} \geq 3$) were performed.

Both T cell types show a stronger directed migration with increasing EF strengths on FN-coated substrates compared to electrotaxis on ICAM1-coated substrates. To further reveal differences in the electrotactic response of the T cells, we analyzed additional motility parameters: migration speed and directionality (Figures 2C and 2D), mean squared displacement (MSD), and velocity autocorrelation (Figures 2E and 2F).

The migration speed of primary human T cells on FN differs significantly compared to T cells on ICAM1-coated substrates (Figures 2C and 2D). Without EF stimulation T cells migrate significantly faster on ICAM1 than T cells on FN-coated substrates (for example with average speed ($\pm$SD) of CD4$^+$ T cells: 12.0 µm/min $\pm$3.0 µm/min (on FN) vs. 19.7 µm/min $\pm$6.2 µm/min (on ICAM1)). When an EF is applied, migration speed increases with increasing EF strength (e.g., average speed ($\pm$SD) for CD4$^+$ T cells on FN: 13.4 µm/min $\pm$3.9 µm/min (100 mV/mm), 18.0 µm/min $\pm$5.7 µm/min (150 mV/mm), 19.7 µm/min $\pm$7.3 µm/min (200 mV/mm)). Migration speed is significantly altered in CD4$^+$ T cells on both coatings ($p < 0.0001$ (FN), $p < 0.0001$ (ICAM1 EF steps 100–200 mV/mm, and $p < 0.05$ (ICAM1 no EF vs. 200 mV/mm), whereas CD8$^+$ T cell migration speed is mainly significantly altered on FN-coated substrates ($p < 0.5 - p < 0.0001$ (on FN) vs. $p < 0.5$ or not significant (on ICAM1)) but less significant than CD4$^+$ T cells (see also Figure S2). T cells show heterogeneity in their migration behavior already without EF stimulation, which we contribute to the cellular heterogeneity of primary human T cells coming from different donors. However, the effect of electrical stimulation on T cell migration is significant compared to the noEF controls shown for each experiment.

The migration directionality increases with increasing EF strength, from 100 to 200 mV/mm. CD8$^+$ T cells show a stronger response measured by migration directionality (CD8$^+$ mean cos(θ): 0.5–0.7) than CD4$^+$ T cells (CD4$^+$ mean cos(θ): 0.2–0.6) (see also Figure S2). Furthermore, additional experiments showed a directed response of CD8$^+$ T cells at 50 mV/mm (see Figure S3), whereas CD4$^+$ T cells show a significantly directed migration from 150 mV/mm for cells on ICAM1 and at 200 mV/mm for cells on FN-coated substrates, indicating a lower EF threshold for electrotaxis in CD8$^+$ than in CD4$^+$ T cells.

The results in Figures 2C–2F further support the observation, that CD8$^+$ T cells have a stronger directional response to the EF cues than CD4$^+$ T cells, which seem less receptive to the EF when considering the migration directionality, the MSD, and the velocity autocorrelation. There is no significant difference between cell migration behavior during the exposure of the EF and after the reversed EF (EFrev). No lag time could be observed within the 10 s frame rate, indicating that T cells sense the field reversal within a time frame shorter than 10 s and adapt their response accordingly.

Velocity autocorrelation (Figures 2E and 2F) was calculated to quantify migration persistence. For both cell types, velocity autocorrelation declines significantly ($p < 0.05$) faster in cells without EF stimulation or with small EF stimulation (no EF and EF $\leq$ 100 mV/mm), indicating a less persistent and more random migration, than cells stimulated with EF strengths of 150 or 200 mV/mm.

The MSD calculates the mean surface area a cell explores over a certain time period, and is a measure of how randomly or efficiently a cell migrates in one direction. MSD curves of CD4$^+$ and CD8$^+$ T cells increase significantly faster ($p < 0.05$) when an EF $\geq$ 100 mV/mm is applied compared to no EF curves (random walk) and further increase with increasing EF strength compared to no EF. This tendency can be observed for both cell types and on both coatings.

At higher EF strength T cells migrate faster, more directed, more persistent and with higher efficiency in the direction toward the anode. Furthermore, electrotactic migration effects are influenced by T cell type and substrate coating.

T cells show electrotaxis toward the anode on collagen-coated substrates and a strong dose-response relationship

To further study the effect of the extracellular environment on T cell electrotaxis, we studied the migration of T cells on 2D collagen-coated substrates (Figure 3) and in 3D collagen gels (Figure 4).

Primary human CD4$^+$ and CD8$^+$ T cells on collagen-coated substrates were exposed to three different EF strengths: 25, 50, and 100 mV/mm. Both cell types show a strongly directed migration toward the anode in an EF (Figure 3). In the absence of EF exposure, T cells on collagen migrate randomly and at a slower speed compared to T cells on FN- or ICAM1-coated substrates (collagen: Figures 3A–3C versus FN and ICAM1; Figures 2A–2D). When exposed to an EF, CD4$^+$ and CD8$^+$ T cell migration speed is significantly increased (CD4$^+$ and CD8$^+$ T cell mean speed (noEF) = 8–9 µm/min, mean speed (25 mV/mm) = 15–17 µm/min, mean speed (50 mV/mm) = 25–30 µm/min, mean speed (100 mV/mm) = 48–56 µm/min) (Figure 3C). Due to the strong electrotactic response of T cells on collagen, smaller EF strengths compared to prior experiments on FN- and ICAM1-coated substrates were applied (25, 50, and 100 mV/mm vs. 100, 150, and 200 mV/mm). CD4$^+$ and CD8$^+$ T cells change migration speed and direction already at 25 mV/mm significantly (CD4$^+$ median cos(θ): noEF $\leq$0.27 vs. 25 mV/mm $\geq$ 0.95; CD8$^+$ median cos(θ): noEF $\leq$0.25 vs. 25 mV/mm $\geq$ 0.86) (Figure 3B). Migration speed and directionality significantly increase with increasing EF strength (Figures 3A–3C).

The analysis of velocity autocorrelation and MSD also show significant differences between T cells exposed to 0 mV/mm (noEF) and T cells exposed to 25, 50, and 100 mV/mm (Figure 3D). Velocity autocorrelation decreases significantly slower for T cells migrating during EF exposure, indicating a more persistent migration compared to no EF (random migration). This effect increases significantly ($p < 0.0001$) with each step of increasing EF strength. The MSD (Figure 3D) of CD4$^+$ and CD8$^+$ T cell migration on collagen-coated substrates also increases significantly ($p < 0.0001$) with increasing EF strength, indicating a highly directed and efficient migration toward the anode.

The electrotactic responses and the dose-response relationship of migration directionality and speed of CD4$^+$ and CD8$^+$ T cells on collagen-coated substrates are significantly stronger, than those observed on FN and ICAM1-coated substrates (Figures 2 and 3). For example, our data shows an increase of CD4$^+$ median cell migration speed (no EF-max EF) for collagen: 7–59 µm/min vs. for FN: 11–19 µm/min and for ICAM1: 17–23 µm/min. Moreover, CD4$^+$ T cell median directionality cos(θ) (0–100 mV/mm) increases: for collagen cos(θ): 0.2–0.9 vs. for FN cos(θ): 0.2–0.7, and for ICAM1 cos(θ): 0.1–0.5.
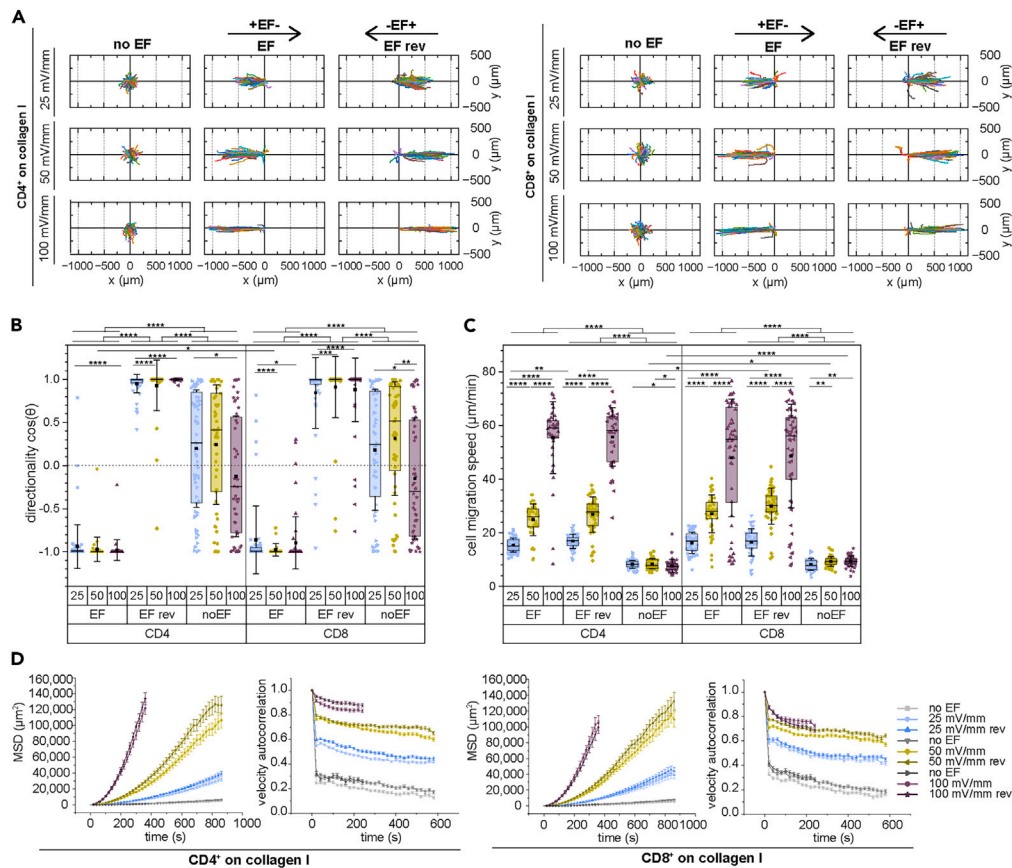
Figure 3. CD4$^+$ and CD8$^+$ T cells migrate toward the anode on collagen-coated substrates

Migration speed and directionality increase significantly with increasing EF strength. Electrotaxis experiments were performed with 3 different EF strengths: 25, 50, and 100 mV/mm, over a total time period of 60 min: 30 min EF and after 30 min EF was reversed (EFrev) (frame rate 10 s).

(A) Migration tracks of CD4$^+$ and CD8$^+$ T cells on collagen I coated substrates over the 30 min time period.

(B and C) Cell migration speed and directionality (error bars are SD), and (D) velocity autocorrelation and mean squared displacement (error bars are SEM) of CD4$^+$ and CD8$^+$ T cells on collagen-coated substrates over 30 min, at the highest applied EF (100 mV/mm) cells were tracked for a shorter time period of 15 min due to fast directed migration. Statistical significance was determined with Mann-Whitney Test (*$p < 0.05$, **$p < 0.01$, ***$p < 0.001$, ****$p < 0.0001$). For all: min. 3 independent experiments (N$_{donors} \geq 3$) were performed.

T cell electrotaxis in 3D collagen gels differs significantly from 2D electrotaxis and depends on the T cell subtype

From our 2D experiments, we found that the protein coating has a significant impact on T cell electrotaxis. However, T cell migration on 2D surfaces is considerably different than migration in 3D environments. To observe cell migration in 3D, cells were embedded into collagen gels and exposed to EFs of two different strengths (50 and 150 mV/mm) (Figure 4). The EF was applied for a total of 3 h, after 1.5 h the polarity was changed (1.5 h of EF, following 1.5 h of EFrev). Cell migration was tracked and analyzed over 1.5 h (= 90 frames) for each condition (noEF, EF, and EFrev) respectively (Figure 4A). T cells migrate significantly slower in 3D collagen gels than on 2D collagen surfaces (CD4$^+$ and CD8$^+$ T cells without EF: mean speed (3D) $\approx$ 4 μm/min; mean speed (2D) $\approx$ 8 μm/min).

In 3D electrotaxis, cell migration directionality (Figure 4B) increases significantly with increasing EF strength, whereas the migration speed is not significantly altered when T cells are exposed to an EF (50–150 mV/mm). However, T cell migration speed is higher in CD4$^+$ T cells (average cell speed CD4$^+$ = 4.7 μm/min) than CD8$^+$ T cells (average cell speed CD8$^+$ = 3.7 μm/min) but only significantly at 50 mV/mm (Figure 4C). In 3D electrotaxis, CD8$^+$ T cells show a stronger directional response (median cos(θ) CD8$^+$ = 0.45 (50 mV/mm) and 0.74 (150 mV/mm)) than CD4$^+$ T cells (median cos(θ) CD4$^+$ = 0.1 (50 mV/mm) and 0.6 (150 mV/mm)) at both EF strengths (Figure 4B) which is in accordance with our observations in the electrotaxis experiments on FN- and ICAM1-coated 2D surfaces. We observed a directed migration of CD4$^+$ and CD8$^+$ T cells toward the anode in all 2D experiments (Figures 2 and 3). Accordingly, CD8$^+$ T cells in 3D collagen gels migrate in the direction toward the anode when an EF of 50 or 150 mV/mm is applied (Figure 4B). They reverse their migration direction after EF reversal. However, CD4$^+$ T cells migrate in the opposite direction in the 3D experiments, toward the cathode, when an EF of 50 or 150 mV/mm is applied. Furthermore, no significant change in migration directionality toward the "new cathode" can be observed when the polarity of the EF is reversed; however, a tendency that the direction of CD4$^+$ T cell migration changes toward lower or slightly negative cos(θ) can be measured (Figure 4B).
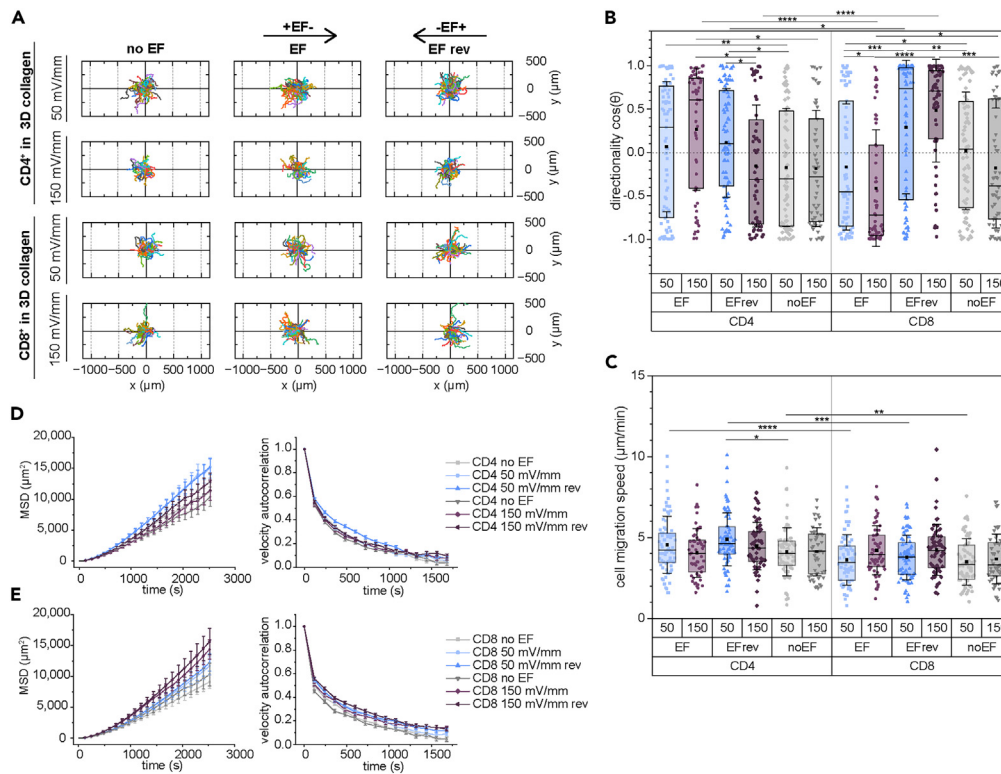
Figure 4. CD4+ and CD8+ T cells show directed migration during EF stimulation in a 3D collagen gel

Migration of CD4+ and CD8+ T cells was observed in a 3D collagen gel with time-lapse microscopy, at two different EF strengths (50 and 150 mV/mm), over a time period of 1.5 h (frame rate 1 min).

(A) Migration tracks of CD4+ and CD8+ T cells over 1.5 h without stimulation (noEF), with EF stimulation (EF), and with reversed EF (EFrev) respectively. CD4+ T cells migrate toward the cathode, whereas CD8+ T cells migrate toward the anode.

(B) Migration directionality and (C) cell migration speed of CD4+ and CD8+ T cells (error bars are SD). Velocity autocorrelation and MSD of CD4+ (D) and CD8+ (E) T cells in a 3D collagen gel (error bars are SEM). Statistical significance was determined with Mann-Whitney Test (*$p < 0.05$, **$p < 0.01$, ***$p < 0.001$, ****$p < 0.0001$). For all: min. 3 independent experiments ($N_{donors} \geq 3$).

The 3D environment has a significant influence on T cell electrotaxis, and a change in migration direction for CD4+ T cells compared to electrotaxis in 2D can be observed. The 3D environment influences the T cell electrotaxis differently depending on the two T cell subtypes.

We further analyzed CD4+ and CD8+ T cell electrotaxis in 3D collagen gels by calculating the MSD and velocity autocorrelation (Figures 4D and 4E). Both characteristics do not seem to be significantly affected by the EF application, compared to the noEF condition. However, MSD and velocity autocorrelation curves show a trend toward directed migration compared to noEF random migration curves. Together with the significant response in migration directionality (Figure 4B) these data support our general observation that T cells show electrotaxis in 3D, but less pronounced compared to 2D environments.

Electric fields do not alter T cell differentiation and viability

EFs cannot only impact cell migration but also influence cell functions.[24,25,38–40] Therefore, we studied the influence of EFs on T cell differentiation, T cell viability, and apoptosis. Phenotypes of electrically stimulated primary human CD4+ and CD8+ T cells were analyzed 3 days after EF exposure (Figures 5A, 5B, and S7).

The following T cell subpopulations were analyzed by flow cytometry: naive (T(N), CD45RO−/CD62L+), effector (T(EFF), CD45RO−/CD62L−), effector memory (T(EM), CD45RO+/CD62L−), and central memory (T(CM), CD45RO+/CD62L+) T cells. Differentiation was analyzed for CD4+ and CD8+ T cells, cultured on FN and ICAM1-coated substrates, stimulated with a small EF strength (50 mV/mm) or a high EF strength (200 mV/mm) for 1 h, and without EF stimulation (noEF) as control.

The application of EFs does not have a significant impact on the mean percentage ratios of T cell subpopulations. However, the percentages of T(EM) and T(EFF) are almost unchanged (1–2%) compared to T(CM) and T(N) subpopulation ratios with EF stimulation (e.g., on FN: CD4+ T(N) decreased from 30% (noEF) to 21% (50 mV/mm) vs. T(CM) increase from 59% (noEF) to 67% (50 mV/mm)). Furthermore, CD4+ T cells show larger differences in T(CM) and T(N) percentage ratios than CD8+ T cells with EF stimulation (e.g., CD4+ T cells on ICAM1 T(CM) increases 5% from no EF to 50 or 200 mV/mm vs. CD8+ increase 0–3% from no EF to 50 or 200 mV/mm). In any case, our results show that electric
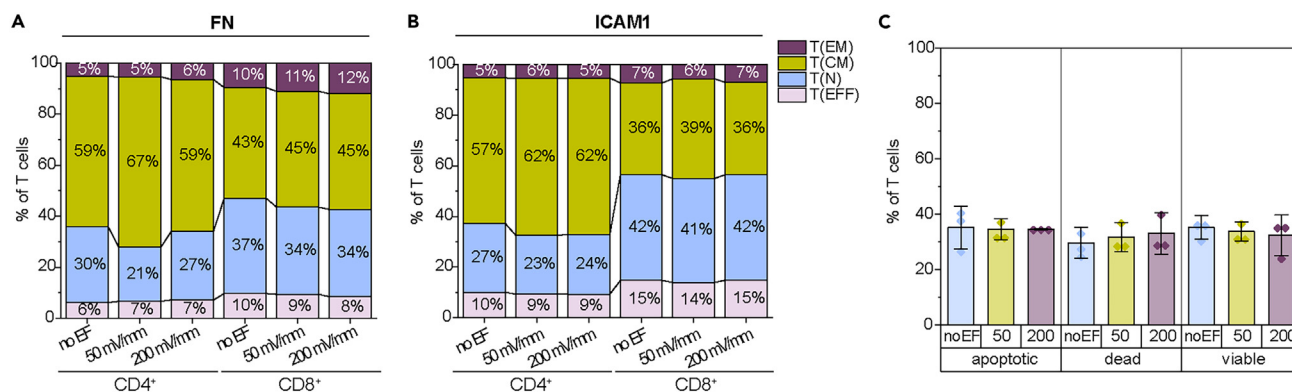
Figure 5. T cell differentiation and viability are not significantly altered by EF stimulation

T cell differentiation was analyzed for CD4$^+$ and CD8$^+$ T cells on (A) FN (N$_{donors}$ = 7) and (B) ICAM1 (N$_{donors}$ ≥ 5) coated substrates, cells were exposed to an EF (0, 50, and 200 mV/mm) for 60 min. Differentiation was analyzed by flow cytometry, 3 days after EF stimulation. T(EM) effector memory, T(CM) central memory, T(N) naive, and T(EFF) effector T cell phenotypes were identified.

(C) CD4$^+$ T cell (cultured on ICAM1-coated substrates) death and apoptosis (Mean ± SD) were analyzed 3 days after EF treatment (0, 50, and 200 mV/mm) (N$_{donors}$ = 3).

stimulation with small electric fields up to 200 mV/mm does not alter T cell differentiation, independent of EF strength, substrate coating, or T cell subtype (Figures 5A and 5B).

To quantify cell viability or apoptosis after EF treatment, T cells were stained with Annexin V and DAPI and analyzed by flow cytometry (Figures 4 and S7). The percentage of apoptotic cells is around 35% with and without EF application (35.2% ± 7.7% (noEF), 34.6% ± 3.8% (50 mV/mm), 34.6% ± 0.3% (200 mV/mm)). The percentage of viable cells is slightly decreased from 35.2% ± 4.3% (noEF) to 32.3% ± 7.4% (200 mV/mm) (Mean ± SD). The percentage of dead, apoptotic, and viable T cells is not significantly influenced by the EF treatment. Thus, EF exposure in the range of 50–200 mV/mm does not damage T cells. Nevertheless, the overall cell viability is rather low since the cells were cultured inside the channel slide of the electrotaxis platform for 3 days (8 days since isolation) until the viability and apoptosis analysis were performed together with differentiation analysis by flow cytometry. Moreover, the cell number inside the channel was optimized for single-cell migration and therefore was lower than the optimal culture condition would require.

DISCUSSION

In our study, we show, that T cell migration is affected by small dc EFs. The electrotactic response depends on the T cell type (CD4$^+$ and CD8$^+$), the substrate coating (FN, ICAM1, collagen I), the electric field strength (25–200 mV/mm), and on the dimensionality of the microenvironment (2D surfaces or 3D gels).

T cells are known for their ability to change between different migration modes, depending on their environment and external stimuli.[6,9,11] T cell migration can be manipulated with small electric fields, but so far only a few studies have been published.[20,25,27,28] In contrast to our study, cathodal migration in T cells was observed on 2D substrates and *in vivo*.[20,25,27,28] A possible explanation is the difference in the used T cell subtypes and the methodologies of how the experiments were performed. Since the effects of T cell type, T cell activation, substrate coating, and the differences of electric field applications e.g., electrode material, agar bridges, or platform design, are very complex, it seems difficult to compare the data on a one-to-one basis.[41] To fully elucidate this phenomenon, more studies are needed.

We show that T cells migrate with increased directionality and migration speed in dc EFs, which is consistent with other findings.[25,27] In addition, we demonstrate, that these T cell responses can differ significantly in their magnitude, depending on the applied EF strength, the T cell subtype, the substrate coating, and in 2D or 3D environments, indicating that native electrotaxis is a complex phenomenon depending on various environmental factors.

Our data show that CD8$^+$ T cells are generally more responsive to the applied EF than CD4$^+$ T cells, meaning electrotaxis can be observed at lower EF strength. Moreover, CD8$^+$ T cell migration direction is overall more significantly changed by EFs, compared to CD4$^+$ T cells. Thus, CD8$^+$ T cells seem to be more sensitive to EF exposure than CD4$^+$ T cells. We hypothesize that this observation could be explained by the heterogeneous CD4$^+$ T cell population. Comprising several different helper subtypes, each CD4$^+$ T cell subtype might show slightly different motility patterns,[42] thus leading to a more heterogeneous electrotaxis response compared to CD8$^+$ T cells, which are supposed to be a more homogeneous T cell population. This observation may show further potential for EFs to differently control T cell migration depending on T cell subtypes. Stronger CD8$^+$ T cell electrotaxis could improve tumor infiltration, which could be beneficial in cancer treatment as CD8$^+$ infiltration is associated with a good prognosis and increased efficacy of immunotherapies.[37] In agreement with our results, electrotaxis of various cell types has been studied, and the effects of EFs were reported to be cell type specific, with even cells from the same lineage showing different directionality during electrotaxis.[21,22] Further, it was reported that T cell migration is influenced by the state of activation, differentiation, and function of the T cell; thus, different T cell subsets respond differently to the same environmental cues.[9,42–44] Since CD4$^+$ and CD8$^+$ T cells

have different responsibilities in the immune system, a differentiated electrical manipulation of the two cell types could be beneficial for the regulation of the immune response and therapeutic use of EFs.

Furthermore, our data show that T cell migration in 2D is strongly influenced by the substrate coating. The migration behavior differed with and without EF application, but differences in migration behavior on the different substrates became more significant when an EF was applied. T cells showed the strongest electrotactic effect in terms of migration directionality and speed, and the highest dose-response relationship on collagen-coated substrates, compared to FN- and ICAM1-coated substrates. However, with EF application cell speed is stronger influenced on FN- than ICAM1-coated substrates, whereas directionality seems not to be significantly affected by FN or ICAM1 coating. However, no change or reorganization of FN, ICAM1, or collagen coating before and after EF application could be observed with immunofluorescence staining before and after EF application. Without EF application, T cells on ICAM1 show the fastest migration, whereas the slowest is observed on collagen-coated substrates. Furthermore, T cells exhibit different cell sizes or adhesion areas on the three different coatings (ICAM1 > FN > collagen). We propose that T cells use different migration modes on FN, ICAM1, and collagen-coated substrates, due to different adhesivity and the different integrins involved in T cell adhesion on the three different protein coatings.[4,40,45–47] Indeed, Jacobelli et al. reported different T cell motility modes dependent on the adhesivity of the substrate. They compared T cell migration on high adhesive ICAM1-coated substrates versus low adhesive blocked substrates without LFA1-ligands.[46] T cells are low adhesive cells, but integrins play a role in T cell migration, especially in 2D.[40,48,49] Different integrins are involved in adhesion and migration on the three different protein coatings studied here, such as the binding of LFA1 (integrin alphaLbeta2) to ICAM1 versus integrin alpha4beta1 and alpha5beta1 binding to FN and integrin alpha1beta1 and alpha2beta1 binding to collagen I.[50–52]

To further study the influence of the microenvironment on T cell electrotaxis, T cell migration was observed in 3D collagen gels. We could not only observe a strong decrease in cell migration speed, but also that directionality was not as strongly influenced as it was by electrotaxis on 2D substrates. Interestingly, we observed different electrotaxis behavior between CD4^{+} and CD8^{+} T cells in the 3D environment. Specifically, the two T cell types migrated in opposite directions when an EF was applied, and CD4^{+} T cells changed their electrotactic migration direction in 3D compared to 2D environments. This change in electrotaxis in different directions suggests different migration modes and cellular differences in the migration mechanisms of CD4^{+} and CD8^{+} T cells in 3D environments. Huang et al. also found that brain tumor-initiating cells can change their migration direction when electrotaxis is studied in 2D and 3D environments. In their studies, they showed a change from anodal cell migration in 2D to cathodal cell migration in 3D. They suggest mechanistic differences between 2D and 3D electrotaxis in terms of PI3K (in 2D) and myosin II contractility (in 3D).[23]

We could further show that CD4^{+} and CD8^{+} T cell differentiation is not significantly influenced by exposure to EFs of physiological strengths independently of the substrate coating. Thus, EFs seem to be a potent stimulus for the manipulation of T cell migration without altering T cell physiology. Additionally, we could not observe a negative impact on T cell viability or an increase in apoptosis after EF exposure.

These results are in accordance with the results published by Arnold et al. They investigated the influence of EF exposure of 150 mV/mm on T cells and observed no significant increase in apoptotic or necrotic T cells.[25] They also further studied T cell parameters after EF exposure (such as cytokine secretion and proliferation), and suggested a broad attenuation of the immune response by EF exposure.[25]

However, it remains to be fully elucidated which cellular mechanisms are involved in the sensing of EFs. It is speculated that similar pathways are involved in chemo- and electrotaxis. EFs are a stimulus that is easy to regulate in its strength and direction, but it is difficult to predict its influence on cellular mechanisms and the microenvironment. It is widely assumed that small EFs do not only alter cellular behavior through their influence on ion channels and cell membrane potentials,[19,24,53–55] but also influence other charged components within the microenvironment. It is assumed that EFs generate ion concentration gradients, electroosmotic flow, and electrophoretic separation of proteins in the microenvironment, which are effects that can be complicated to fully estimate and thoroughly define in terms of their underlying molecular mechanisms.[19,53,56]

In summary, the results of our study demonstrate that physiological strength dc EFs have no negative influence on primary human CD4^{+} and CD8^{+} T cell differentiation and viability, but present a potent stimulus to direct T cell migration dependent on the T cell subtype (CD4^{+} or CD8^{+}), applied EF strength, substrate coating, and in 2D or 3D environments. Keeping this in mind, EFs present an effective physical stimulus to direct T cell migration in various 2D and 3D environments, and even in vivo as shown by Lin et al..[28] As the electrotactic responses are differing, depending on the T cell subtype and the microenvironment, EFs have the potential to guide T cell migration in different directions or with different migration speeds. These effects could be further studied in more complex microenvironments to better mimic the conditions in vivo, e.g., using tumor microenvironments or organoids.[57] Furthermore, it is important to elucidate the impact of endogenous tumor EFs on T cells, specifically on engineered or cytotoxic T cells to improve T cell-based tumor therapies. The ability of exogenous EFs to reliably guide the T cell migration of different T cell subtypes differentially, would allow to modulate (improve or limit) the access of T cells to specific tissues. Due to strong electrotactic cell response, even overriding chemotactic stimuli, EFs might offer the possibility to improve T cell migration and infiltration specifically into solid and "cold" tumors. By guiding specifically CD8^{+} T cells and engineered T cells efficiently into the tumor, EFs could improve the effectiveness of immunotherapies against solid and immunosuppressive cancers. In future therapeutic applications, in diseases where the immune system and T cell activity are malfunctioned (e.g., inflammatory and autoimmune disorders), EFs could further help to control the immune response.

Limitations of the study

In conclusion, we demonstrate that EFs present an effective physical stimulus to direct T cell migration in various 2D and 3D environments. The results of our study demonstrate that physiological strength dc EFs have no negative influence on primary human CD4^{+} and CD8^{+} T cell

differentiation and viability, but present a potent stimulus to direct T cell migration dependent on the T cell subtype (CD4$^+$ or CD8$^+$), applied EF strength, substrate coating, and in 2D or 3D environments. However, we showed partially opposite results of electrotaxis direction, compared to previously published studies, illustrating the complexity of electrotaxis experiments and the unpredictable influences of different experimental set-ups, limiting the comparability of electrotaxis studies without standardized experimental parameters. EFs are a complex physical stimulus that impact all charged molecules in their surroundings. Thus, it is difficult to predict its influence on cellular mechanisms and the microenvironment. Therefore, these effects should be further studied in more complex microenvironments to better mimic the conditions *in vivo* and to elucidate the behavior of integrins and other membrane and cytoskeletal proteins in an EF and their involvement in electrotaxis. Moreover, it remains to be fully elucidated which cellular mechanisms are involved in the sensing of EFs. Furthermore, deeper insight into the underlying molecular mechanisms of T cell electrotaxis is needed and should be studied more extensively in the future. We believe that this will be crucial for the further development of therapeutic applications.

STAR★METHODS

Detailed methods are provided in the online version of this paper and include the following:

- KEY RESOURCES TABLE
- RESOURCE AVAILABILITY
  - Lead contact
  - Materials availability
  - Data and code availability
- EXPERIMENTAL MODEL AND STUDY PARTICIPANT DETAILS
  - Primary human T cells
- METHOD DETAILS
  - T cell isolation and activation
  - T cell migration experiments
  - Electric field application
  - Cell imaging and analysis
  - Migration speed and directionality analysis
  - Mean squared displacement (MSD) and autocorrelation analysis
  - Flow cytometry
  - T cell differentiation
  - T cell viability and apoptosis
- QUANTIFICATION AND STATISTICAL ANALYSIS
  - Data treatment and statistical analysis

SUPPLEMENTAL INFORMATION

Supplemental information can be found online at https://doi.org/10.1016/j.isci.2024.109746.

AUTHOR CONTRIBUTIONS

Conceptualization, R.K., J.G., and K.E; methodology K.E.; formal analysis and investigation, K.E. and F.S.; writing-original draft preparation, K.E.; writing—review and editing, R.K., J.G. and K.E.; visualization, K.E.; supervision, R.K. and J.G.; funding acquisition, R.K. and J.G. All authors have read and agreed to the published version of the article.

DECLARATION OF INTERESTS

The authors declare no conflicts of interest.

REFERENCES

1. Vicente-Manzanares, M., Webb, D.J., and Horwitz, A.R. (2005). Cell migration at a glance. J. Cell Sci. *118*, 4917–4919. https://doi.org/10.1242/jcs.02662.

2. Bear, J.E., and Haugh, J.M. (2014). Directed migration of mesenchymal cells: where signaling and the cytoskeleton meet. Curr. Opin. Cell Biol. *30*, 74–82. https://doi.org/10.1016/j.ceb.2014.06.005.

3. SenGupta, S., Parent, C.A., and Bear, J.E. (2021). The principles of directed cell migration. Nat. Rev. Mol. Cell Biol. *22*, 529–547. https://doi.org/10.1038/s41580-021-00366-6.

4. Lämmermann, T., and Sixt, M. (2009). Mechanical modes of 'amoeboid' cell migration. Curr. Opin. Cell Biol. *21*, 636–644. https://doi.org/10.1016/j.ceb.2009.05.003.

5. Reversat, A., Gaertner, F., Merrin, J., Stopp, J., Tasciyan, S., Aguilera, J., de Vries, I., Hauschild, R., Hons, M., Piel, M., et al. (2020). Cellular locomotion using environmental topography. Nature *582*, 582–585. https://doi.org/10.1038/s41586-020-2283-z.

6. Kameritsch, P., and Renkawitz, J. (2020). Principles of Leukocyte Migration Strategies. Trends Cell Biol. *30*, 818–832. https://doi.org/10.1016/j.tcb.2020.06.007.

7. Yamada, K.M., and Sixt, M. (2019). Mechanisms of 3D cell migration. Nat. Rev. Mol. Cell Biol. *20*, 738–752. https://doi.org/10.1038/s41580-019-0172-9.

8. Lämmermann, T., and Germain, R.N. (2014). The multiple faces of leukocyte interstitial migration. Semin. Immunopathol. *36*, 227–251. https://doi.org/10.1007/s00281-014-0418-8.

9. Krummel, M.F., Bartumeus, F., and Gérard, A. (2016). T cell migration, search strategies and mechanisms. Nat. Rev. Immunol. *16*, 193–201. https://doi.org/10.1038/nri.2015.16.

10. Paluch, E.K., Aspalter, I.M., and Sixt, M. (2016). Focal Adhesion-Independent Cell Migration. Annu. Rev. Cell Dev. Biol. *32*, 469–490. https://doi.org/10.1146/annurev-cellbio-111315-125341.

11. Gaylo, A., Schrock, D.C., Fernandes, N.R.J., and Fowell, D.J. (2016). T Cell Interstitial Migration: Motility Cues from the Inflamed Tissue for Micro- and Macro-Positioning. Front. Immunol. *7*, 428. https://doi.org/10.3389/fimmu.2016.00428.

12. Khachaturyan, G., Holle, A.W., Ende, K., Frey, C., Schwederski, H.A., Eiseler, T., Paschke, S., Micoulet, A., Spatz, J.P., and Kemkemer, R. (2022). Temperature-sensitive migration dynamics in neutrophil-differentiated HL-60 cells. Sci. Rep. *12*, 7053. https://doi.org/10.1038/s41598-022-10858-w.

13. Rajnicek, A.M., Foubister, L.E., and McCaig, C.D. (2007). Prioritising guidance cues: directional migration induced by substratum contours and electrical gradients is controlled by a rho/cdc42 switch. Dev. Biol. *312*, 448–460. https://doi.org/10.1016/j.ydbio.2007.09.051.

14. McCaig, C.D., Rajnicek, A.M., Song, B., and Zhao, M. (2005). Controlling cell behavior electrically: current views and future potential. Physiol. Rev. *85*, 943–978. https://doi.org/10.1152/physrev.00020.2004.

15. Foulds, I.S., and Barker, A.T. (1983). Human skin battery potentials and their possible role in wound healing. Br. J. Dermatol. *109*, 515–522. https://doi.org/10.1111/j.1365-2133.1983.tb07673.x.

16. Levin, M., Pezzulo, G., and Finkelstein, J.M. (2017). Endogenous Bioelectric Signaling Networks: Exploiting Voltage Gradients for Control of Growth and Form. Annu. Rev. Biomed. Eng. *19*, 353–387. https://doi.org/10.1146/annurev-bioeng-071114-040647.

17. Zhu, K., Hum, N.R., Reid, B., Sun, Q., Loots, G.G., and Zhao, M. (2020). Electric Fields at Breast Cancer and Cancer Cell Collective Galvanotaxis. Sci. Rep. *10*, 8712. https://doi.org/10.1038/s41598-020-65566-0.

18. Nuccitelli, R., Nuccitelli, P., Li, C., Narsing, S., Pariser, D.M., and Lui, K. (2011). The electric field near human skin wounds declines with age and provides a noninvasive indicator of wound healing. Wound Repair Regen. *19*, 645–655. https://doi.org/10.1111/j.1524-475X.2011.00723.x.

19. Cortese, B., Palamà, I.E., D'Amone, S., and Gigli, G. (2014). Influence of electrotaxis on cell behaviour. Integr. Biol. *6*, 817–830. https://doi.org/10.1039/c4ib00142g.

20. Li, J., Zhu, L., Zhang, M., and Lin, F. (2012). Microfluidic device for studying cell migration in single or co-existing chemical gradients and electric fields. Biomicrofluidics *6*, 24121–2412113. https://doi.org/10.1063/1.4718721.

21. Ferrier, J., Ross, S.M., Kanehisa, J., and Aubin, J.E. (1986). Osteoclasts and osteoblasts migrate in opposite directions in response to a constant electrical field. J. Cell. Physiol. *129*, 283–288. https://doi.org/10.1002/jcp.1041290303.

22. Hoare, J.I., Rajnicek, A.M., McCaig, C.D., Barker, R.N., and Wilson, H.M. (2016). Electric fields are novel determinants of human macrophage functions. J. Leukoc. Biol. *99*, 1141–1151. https://doi.org/10.1189/jlb.3A0815-390R.

23. Huang, Y.-J., Hoffmann, G., Wheeler, B., Schiapparelli, P., Quinones-Hinojosa, A., and Searson, P. (2016). Cellular microenvironment modulates the galvanotaxis of brain tumor initiating cells. Sci. Rep. *6*, 21583. https://doi.org/10.1038/srep21583.

24. Thrivikraman, G., Boda, S.K., and Basu, B. (2018). Unraveling the mechanistic effects of electric field stimulation towards directing stem cell fate and function: A tissue engineering perspective. Biomaterials *150*, 60–86. https://doi.org/10.1016/j.biomaterials.2017.10.003.

25. Arnold, C.E., Rajnicek, A.M., Hoare, J.I., Pokharel, S.M., McCaig, C.D., Barker, R.N., and Wilson, H.M. (2019). Physiological strength electric fields modulate human T cell activation and polarisation. Sci. Rep. *9*, 17604. https://doi.org/10.1038/s41598-019-53898-5.

26. Franke, K., and Gruler, H. (1990). Galvanotaxis of human granulocytes: electric field jump studies. Eur. Biophys. J. *18*, 335–346. https://doi.org/10.1007/BF00196924.

27. Li, J., Nandagopal, S., Wu, D., Romanuik, S.F., Paul, K., Thomson, D.J., and Lin, F. (2011). Activated T lymphocytes migrate toward the cathode of DC electric fields in microfluidic devices. Lab Chip *11*, 1298–1304. https://doi.org/10.1039/c0lc00371a.

28. Lin, F., Baldessari, F., Gyenge, C.C., Sato, T., Chambers, R.D., Santiago, J.G., and Butcher, E.C. (2008). Lymphocyte electrotaxis in vitro and in vivo. J. Immunol. *181*, 2465–2471. https://doi.org/10.4049/jimmunol.181.4.2465.

29. Ostroumov, D., Fekete-Drimusz, N., Saborowski, M., Kühnel, F., and Woller, N. (2018). CD4 and CD8 T lymphocyte interplay in controlling tumor growth. Cell. Mol. Life Sci. *75*, 689–713. https://doi.org/10.1007/s00018-017-2686-7.

30. Tay, R.E., Richardson, E.K., and Toh, H.C. (2021). Revisiting the role of CD4+ T cells in cancer immunotherapy-new insights into old paradigms. Cancer Gene Ther. *28*, 5–17. https://doi.org/10.1038/s41417-020-0183-x.

31. Yates, K.B., Tonnerre, P., Martin, G.E., Gerdemann, U., Al Abosy, R., Comstock, D.E., Weiss, S.A., Wolski, D., Tully, D.C., Chung, R.T., et al. (2021). Epigenetic scars of CD8+ T cell exhaustion persist after cure of chronic infection in humans. Nat. Immunol. *22*, 1020–1029. https://doi.org/10.1038/s41590-021-00979-1.

32. Zhu, J., Yamane, H., and Paul, W.E. (2010). Differentiation of effector CD4 T cell populations (*). Annu. Rev. Immunol. *28*, 445–489. https://doi.org/10.1146/annurev-immunol-030409-101212.

33. Labanieh, L., and Mackall, C.L. (2023). CAR immune cells: design principles, resistance and the next generation. Nature *614*, 635–648. https://doi.org/10.1038/s41586-023-05707-3.

34. Newick, K., O'Brien, S., Moon, E., and Albelda, S.M. (2017). CAR T Cell Therapy for Solid Tumors. Annu. Rev. Med. *68*, 139–152. https://doi.org/10.1146/annurev-med-062315-120245.

35. van der Woude, L.L., Gorris, M.A.J., Halilovic, A., Figdor, C.G., and de Vries, I.J.M. (2017). Migrating into the Tumor: A Roadmap for T Cells. Trends Cancer *3*, 797–808. https://doi.org/10.1016/j.trecan.2017.09.006.

36. Vignali, D., and Kallikourdis, M. (2017). Improving homing in T cell therapy. Cytokine Growth Factor Rev. *36*, 107–116. https://doi.org/10.1016/j.cytogfr.2017.06.009.

37. Kuczek, D.E., Larsen, A.M.H., Thorseth, M.-L., Carretta, M., Kalvisa, A., Siersbæk, M.S., Simões, A.M.C., Roslind, A., Engelholm, L.H., Noessner, E., et al. (2019). Collagen density regulates the activity of tumor-infiltrating T cells. J. Immunother. Cancer 7, 68. https://doi.org/10.1186/s40425-019-0556-6.

38. Banks, T.A., Luckman, P.S.B., Frith, J.E., and Cooper-White, J.J. (2015). Effects of electric fields on human mesenchymal stem cell behaviour and morphology using a novel multichannel device. Integr. Biol. 7, 693–712. https://doi.org/10.1039/c4ib00297k.

39. Li, C., Levin, M., and Kaplan, D.L. (2016). Bioelectric modulation of macrophage polarization. Sci. Rep. 6, 21044. https://doi.org/10.1038/srep21044.

40. Hons, M., Kopf, A., Hauschild, R., Leithner, A., Gaertner, F., Abe, J., Renkawitz, J., Stein, J.V., and Sixt, M. (2018). Chemokines and integrins independently tune actin flow and substrate friction during intranodal migration of T cells. Nat. Immunol. 19, 606–616. https://doi.org/10.1038/s41590-018-0109-z.

41. Meng, S., Rouabhia, M., and Zhang, Z. (2021). Electrical Stimulation and Cellular Behaviors in Electric Field in Biomedical Research. Materials 15, 165. https://doi.org/10.3390/ma15010165.

42. Gaylo-Moynihan, A., Prizant, H., Popović, M., Fernandes, N.R.J., Anderson, C.S., Chiou, K.K., Bell, H., Schrock, D.C., Schumacher, J., Capece, T., et al. (2019). Programming of Distinct Chemokine-Dependent and -Independent Search Strategies for Th1 and Th2 Cells Optimizes Function at Inflamed Sites. Immunity 51, 298–309.e6. https://doi.org/10.1016/j.immuni.2019.06.026.

43. Mandl, J.N., Liou, R., Klauschen, F., Vrisekoop, N., Monteiro, J.P., Yates, A.J., Huang, A.Y., and Germain, R.N. (2012). Quantification of lymph node transit times reveals differences in antigen surveillance strategies of naive CD4+ and CD8+ T cells. Proc. Natl. Acad. Sci. USA 109, 18036–18041. https://doi.org/10.1073/pnas.1211717109.

44. Gebhardt, T., Whitney, P.G., Zaid, A., Mackay, L.K., Brooks, A.G., Heath, W.R., Carbone, F.R., and Mueller, S.N. (2011). Different patterns of peripheral migration by memory CD4+ and CD8+ T cells. Nature 477, 216–219. https://doi.org/10.1038/nature10339.

45. Oakes, P.W., and Fowell, D.J. (2018). CCR7 fuels and LFA-1 grips. Nat. Immunol. 19, 516–518. https://doi.org/10.1038/s41590-018-0118-y.

46. Jacobelli, J., Bennett, F.C., Pandurangi, P., Tooley, A.J., and Krummel, M.F. (2009). Myosin-IIA and ICAM-1 regulate the interchange between two distinct modes of T cell migration. J. Immunol. 182, 2041–2050. https://doi.org/10.4049/jimmunol.0803267.

47. Hogg, N., Laschinger, M., Giles, K., and McDowall, A. (2003). T-cell integrins: more than just sticking points. J. Cell Sci. 116, 4695–4705. https://doi.org/10.1242/jcs.00876.

48. Katakai, T., Habiro, K., and Kinashi, T. (2013). Dendritic cells regulate high-speed interstitial T cell migration in the lymph node via LFA-1/ICAM-1. J. Immunol. 191, 1188–1199. https://doi.org/10.4049/jimmunol.1300739.

49. Lämmermann, T., Bader, B.L., Monkley, S.J., Worbs, T., Wedlich-Söldner, R., Hirsch, K., Keller, M., Förster, R., Critchley, D.R., Fässler, R., and Sixt, M. (2008). Rapid leukocyte migration by integrin-independent flowing and squeezing. Nature 453, 51–55. https://doi.org/10.1038/nature06887.

50. Bertoni, A., Alabiso, O., Galetto, A.S., and Baldanzi, G. (2018). Integrins in T Cell Physiology. Int. J. Mol. Sci. 19, 485. https://doi.org/10.3390/ijms19020485.

51. Smith, A., Bracke, M., Leitinger, B., Porter, J.C., and Hogg, N. (2003). LFA-1-induced T cell migration on ICAM-1 involves regulation of MLCK-mediated attachment and ROCK-dependent detachment. J. Cell Sci. 116, 3123–3133. https://doi.org/10.1242/jcs.00606.

52. Guasch, J., Muth, C.A., Diemer, J., Riahinezhad, H., and Spatz, J.P. (2017). Integrin-Assisted T-Cell Activation on Nanostructured Hydrogels. Nano Lett. 17, 6110–6116. https://doi.org/10.1021/acs.nanolett.7b02636.

53. Allen, G.M., Mogilner, A., and Theriot, J.A. (2013). Electrophoresis of cellular membrane components creates the directional cue guiding keratocyte galvanotaxis. Curr. Biol. 23, 560–568. https://doi.org/10.1016/j.cub.2013.02.047.

54. Zhao, S., Mehta, A.S., and Zhao, M. (2020). Biomedical applications of electrical stimulation. Cell. Mol. Life Sci. 77, 2681–2699. https://doi.org/10.1007/s00018-019-03446-1.

55. Ozkucur, N., Perike, S., Sharma, P., and Funk, R.H.W. (2011). Persistent directional cell migration requires ion transport proteins as direction sensors and membrane potential differences in order to maintain directedness. BMC Cell Biol. 12, 4. https://doi.org/10.1186/1471-2121-12-4.

56. Chernet, B., and Levin, M. (2013). Endogenous Voltage Potentials and the Microenvironment: Bioelectric Signals that Reveal, Induce and Normalize Cancer. J. Clin. Exp. Oncol. S1-002. https://doi.org/10.4172/2324-9110.S1-002.

57. Castellote-Borrell, M., Merlina, F., Rodríguez, A.R., and Guasch, J. (2023). Biohybrid Hydrogels for Tumoroid Culture. Adv. Biol. 7, e2300118. https://doi.org/10.1002/adbi.202300118.

58. Gorelik, R., and Gautreau, A. (2014). Quantitative and unbiased analysis of directional persistence in cell migration. Nat. Protoc. 9, 1931–1943. https://doi.org/10.1038/nprot.2014.131.

59. E. Meijering, O. Dzyubachyk, and I. Smal, eds. (2012). Methods in enzymology: Imaging and spectroscopic analysis of living cells (Elsevier/Academic Press).

60. Del Pérez Río, E., Santos, F., Rodriguez Rodriguez, X., Martínez-Miguel, M., Roca-Pinilla, R., Arís, A., Garcia-Fruitós, E., Veciana, J., Spatz, J.P., Ratera, I., et al. (2020). CCL21-loaded 3D hydrogels for T cell expansion and differentiation. Biomaterials 259, 120313. https://doi.org/10.1016/j.biomaterials.2020.120313.

61. Del Pérez Río, E., Martinez Miguel, M., Veciana, J., Ratera, I., and Guasch, J. (2018). Artificial 3D Culture Systems for T Cell Expansion. ACS Omega 3, 5273–5280. https://doi.org/10.1021/acsomega.8b00521.

62. Santos, F., Valderas-Gutiérrez, J., Del Pérez Río, E., Castellote-Borrell, M., Rodriguez, X.R., Veciana, J., Ratera, I., and Guasch, J. (2022). Enhanced human T cell expansion with inverse opal hydrogels. Biomater. Sci. 10, 3730–3738. https://doi.org/10.1039/D2BM00486K.

STAR★METHODS

KEY RESOURCES TABLE

REAGENT or RESOURCE	SOURCE	IDENTIFIER
Antibodies		
Anti-human CD3 mouse IgG2aκ - FITC	Miltenyi Biotec	Cat#: 130-113-128 Lot: 520080617
Anti-human CD4 recombinant human IgG1 - APC	Miltenyi Biotec	Cat#: 130-113-784 Lot: 5200908342
Anti-human CD8 recombinant human IgG1 - APC	Miltenyi Biotec	Cat#: 130-110-817 Lot: 5200908333
Anti-human CD45RO mouse IgG2a - FITC	ImmunoTools	Cat#: 21336453 Lot: 277066
Anti-human CD62L mouse IgG1κ - PE	BioLegend	Cat#: 304805 Lot: B311805
Mouse IgG2a isotype control - FITC	Miltenyi Biotec	Cat#: 130-113-271 Lot: 5200908299
REA control recombinant human IgG1- APC	Miltenyi Biotec	Cat#: 130-113-434 Lot: 5200900805
Mouse IgG2a isotype control - FITC	ImmunoTools	Cat#: 21275523 Lot: 276940
Mouse IgG1k isotype control - PE	BioLegend	Cat#: 400111 Lot: B314064
Biological samples		
Human buffy coat from healthy male blood donors (for T cell isolation)	Institute for Clinical Transfusion Medicine in Tübingen, Germany	N/A
Chemicals, peptides, and recombinant proteins		
Bovine Collagen I (5 mg/mL)	Viscofan	Cat# 500060635
Annexin V - FITC	Miltenyi Biotec	Cat# 130-097-928
Dynabeads human T-Activator CD3/CD28	Gibco	Cat# 11131D
Human FN (fibronectin) (1 mg/mL)	Gibco	Cat# PHE0023
Human ICAM1 (intercellular adhesion molecule 1) (200 μg/mL)	Invitrogen	Cat# A42523
Human IL-2 (interleukin-2)	Miltenyi Biotec	Cat# 130-097-744
Critical commercial assays		
MACS negative isolation kits for $CD4^+$ / $CD8^+$ T cells	Miltenyi Biotec	Cat# 130-096-533; Cat# 130-096-495
Software and algorithms		
Excel Macro DiPer	Gorelik et al.[58]	https://doi.org/10.1038/nprot.2014.131
ImageJ	NIH	https://imagej.net/ij/
ImageJ macro MTrackJ	Meijering et al.[59]	https://imagescience.org/meijering/software/mtrackj/
OriginPro	OriginLab	https://www.originlab.com/
Flowing Software	Turku Center for Biotechnology	https://bioscience.fi/services/cell-imaging/flowing-software/
FlowJo	FlowJo LLC, BD	https://www.flowjo.com/flowing soft
Other		
Ibidi μ-slide I (0.4 mm, ibiTreat)	ibidi	Cat# 80106

RESOURCE AVAILABILITY

Lead contact

Further information and requests for resources and reagents should be directed to and will be fulfilled by the lead contact, Ralf Kemkemer (ralf.kemkemer@reutlingen-university.de; ralf.kemkemer@mr.mpg.de).

Materials availability

This study did not generate new unique reagents.

Data and code availability

- All data reported in this paper will be shared by the lead contact upon request.
- This paper does not report original code.
- Any additional information required to reanalyze the data reported in this paper is available from the lead contact upon request.

EXPERIMENTAL MODEL AND STUDY PARTICIPANT DETAILS

Primary human T cells

Primary human CD4$^+$ and CD8$^+$ T cells were isolated from human buffy coats from healthy male blood donors. Buffy Coats were supplied by the Centre for Clinical Transfusion Medicine in Tübingen (Germany) after the ethical approval of the ethics committee of the University Clinic Tübingen (Germany).

METHOD DETAILS

T cell isolation and activation

Primary human CD4$^+$ and CD8$^+$ T cells were isolated from human buffy coats from healthy male blood donors, using a previously described protocol.[52,60–62] Buffy Coats were supplied by the Centre for Clinical Transfusion Medicine in Tübingen (Germany) after the ethical approval of the ethics committee of the University Clinic Tübingen (Germany). Peripheral blood mononucleated cells (PBMCs) were isolated by density gradient centrifugation with Lymphoprep (Stemcell technologies). T cells were isolated from PBMCs by negative magnetic activated cell sorting (MACS) using CD4$^+$ and CD8$^+$ T cell isolation Kits (Miltenyi Biotec). Cell purity was confirmed by flow cytometry, T cells were stained with anti-human CD3-FITC and anti-human CD4-APC or anti-human CD8-APC antibodies, and respective controls (all Miltenyi Biotec) cells were gated for viable cells and analyzed for FITC and APC fluorescence. Cells of purity >90% (usually >95%) were used for experiments. T cells were activated according to manufacturers' protocol with Dynabeads, human T-Activator CD3/CD28 (Invitrogen), in a 1:1 (bead : cell) ratio, 30 U/mL interleukin-2 (IL-2) (Miltenyi Biotec) in supplemented cell culture medium (10% fetal bovine serum (FBS) and 1% penicillin/streptomycin (P/S) in RPMI 1640 GlutaMAX) (all Gibco) and cultured at 37°C, 5% CO$_2$, and high humidity in a cell culture incubator. After 3 days, Dynabeads were removed from the cell suspension with a magnet, dead cells were removed by centrifugation and T cells were seeded for experiments.

T cell migration experiments

For all experiments (except 3D collagen gels), channel slides (μ-slide I ibiTreat (Ibidi)) were coated with 100 μL of either 10 μg/mL human fibronectin (FN) diluted in DPBS (both Gibco), 1 μg/mL human ICAM1 (Invitrogen) diluted in DPBS (Gibco), or 1.5 mg/mL bovine collagen I (Viscofan) diluted in 0.1% acetic acid (Carl Roth), for 4 hours at 37°C. Channel slides were washed 3 times with DPBS (Gibco) before 50,000 T cells were seeded inside the channel, and 500 μL of supplemented RPMI media was added to each reservoir of the channel slide. T cells were left to adhere for 17 hours inside the cell culture incubator (37°C, 5% CO$_2$, high humidity) before experiments were started.

For migration experiments in 3D collagen gels, a collagen gel with a final concentration of 1.5 mg/mL was freshly prepared of 51 μL gel neutralization solution (20% RPMI 1640 10x (Sigma Aldrich), 1% P/S (Gibco), 2% GlutaMAX (Gibco), 25mM HEPES (Gibco), 0.002% folic acid (Sigma Aldrich), 0.4% NaHCO3 (Sigma Aldrich), in sterile ddH2O), 4 μL 1M NaOH (Th. Geyer), and 45 μL bovine collagen I (5 mg/mL, Viscofan). Then 50 μL cell suspension of a concentration of 10^6 cells/mL (= 50,000 cells) was added, to the gel-mix, and pipetted into the channel slide. For polymerization, the gel-cell mix was left in the incubator (37°C) for 30 min before 1 mL of supplemented cell culture media was added to each of the channel reservoirs. Electric field experiments were started 3 hours after cell seeding.

Electric field application

EF stimulation of T cells was performed in an electrotaxis platform (see Figure S8) using modified channel slides (μ-slide I ibiTreat (Ibidi)) with channel dimensions 50 x 5 x 0.4 mm (l x w x h)) similar to Arnold et al.[25] Two reservoirs for PBS were additionally glued next to the slide. The reservoirs of the channel were filled with 1 mL cell culture medium and connected to the PBS reservoirs with agar-salt bridges (glass tubes: length: 50 mm, inner diameter: 2 mm, and filled with 2% agarose-PBS gel). Silver/silver chloride electrodes (electrochemical deposition AgCl on silver foil for 10 min at 10 mA in 1M hydrochloric acid) were inserted in the PBS reservoirs and connected to the direct current power source and an amperemeter. The EF strength inside the channels was determined by measuring the voltage with a voltmeter between two platinum electrodes (platinum wire), one at each end of the channel. Electric current and voltage were measured throughout the whole experiment.

T cells inside the channel slides were exposed to a direct current electric field (dc EF) for 60 min in total, for 2D experiments, and for 3 hours in total for experiments in 3D collagen gels. After half of the time of the EF exposure, the polarity of the supply voltage was changed, and the direction of the EF was reversed (EF rev). Prior to the EF treatment, cells were observed for 1-1.5 hours without EF (noEF) as control. Therefore, cell migration at noEF, EF and EFrev, can be directly compared (all 3 conditions are performed with the same set-up and cells). Time-lapse movies were recorded over the whole duration of the experiment. The EF was set up with the anode (positive pole) to the left of the electro-taxis chambers and was then changed to the right when the EF was reversed.

Cell imaging and analysis

Time-lapse video microscopy was performed with standard inverted cell culture microscopes (Axiovert Zeiss or Olympus CKX 53, equipped with a camera AxioCam105color (Zeiss), 10x phase contrast objective) inside a cell culture incubator (5% CO_2, 37°C, and high humidity). Images were taken at a frame rate of 10 s for 2D experiments or 1 min for 3D experiments, and every second image was analyzed (analyzed frame rate: 20 s for 2D, for 3D: 2 min).

Cells were tracked manually with the macro MTrackJ[59] provided by ImageJ (NIH). For each condition and each experiment ($N_{donors} \geq 3$), at least 10 - 20 cells were tracked ($N_{cells\ analyzed} >30$, usually >45). All motile cells that remained in the observation area throughout the 30 min time-period (90 frames) were analyzed for noEF, EF, and EFrev conditions respectively. Except for experiments on 2D collagen at 100 mV/mm: 15 min (45 frames), and 3D experiments: 90 min (45 frames) were analyzed. X- and Y-coordinates from cell tracks were transferred from ImageJ into Excel for further data processing. All graphs were created in OriginPro (OriginLab).

Migration speed and directionality analysis

Migration speed was calculated with the total migration track length, divided by the total migration time period for each condition (over 30 min for FN and ICAM1, over 15 min for collagen I, and 90 min for 3D experiments).

Migration directionality was calculated as the cosine of the angle (θ) between the straight line between the first and the last point of the migration track and the X-axis (parallel to the EF vector). The cosine values lie between +1 and -1. Cells moving very directed toward the left would have a directedness of -1, whereas cells moving to the right would have a directedness of +1. A value of 0 indicates random migration.

Mean squared displacement (MSD) and autocorrelation analysis

To evaluate directional persistence over increasing time intervals and migration efficiency at different EF strengths in T cells, MSD analysis was performed on the tracked cell migration data. MSD is calculated over 1/2 of the migration time for each condition using the program MSD available in DiPer Excel macro provided by Gorelik et al.[58] MSD relates to the average surface area explored by the cells in a given time interval.

To evaluate directional persistence at different EF strengths in T cells, velocity autocorrelation analysis was performed on the data of the cell migration tracks. Normalized velocity autocorrelation approximates the direction autocorrelation and was computed over 1/3 of the migration track for each condition using the program Vel.Cor available in DiPer excel macro provided by Gorelik et al.[58] The analysis produces decaying curves, and the rate at which these curves decay reflects how much a cell changes its migration direction.

Flow cytometry

Flow cytometry experiments were performed with a BD FACS Canto II (BD Biosciences) of the FACS Core Facility Berg at the University Clinic Tübingen. For cell purity measurements, a FACS buffer of DPBS with 0.5% bovine serum albumin (BSA), 2 mM EDTA was used. For all other measurements, a FACS buffer of DPBS with 0.1% FCS was used. Analysis of flow cytometry data was performed with Flowing Software (Turku Center for Biotechnology) or FlowJo software (FlowJo LLC, BD).

T cell differentiation

For T cell differentiation experiments, T cells were stained 3 days after EF stimulation with anti-human CD45RO-FITC (Immunotools) and CD62L-PE (BioLegend), and the corresponding controls. T cells were washed out of the channel slides, cells were resuspended in 50 μL FACS buffer and incubated with antibodies for 30 min on ice, in the dark. After washing cells with FACS buffer, cells were gated with SSC-A vs. FSC-A for living cells and analyzed for FITC and PE fluorescence by flow cytometry. Quadrants were defined by positive and negative/control PE and FITC signals.

T cell viability and apoptosis

For cell viability and apoptosis measurements, 3 days after EF treatment on ICAM 1 coated substrates $CD4^+$ T cells were stained with Annexin V-FITC in Annexin binding buffer (both Miltenyi Biotec) for 15 min at room temperature, according to the manufacturer's protocol. Cells were washed and resuspended in FACS buffer. Prior to flow cytometry measurements, DAPI (Miltenyi Biotec) was added and cells were gated for dead and alive cells (excluding cell debris) with SSC-A vs. FSC-A and analyzed for DAPI and FITC-fluorescence. Quadrants of viable, apoptotic, and dead cell populations were defined by positive and negative/control DAPI and FITC signals.

QUANTIFICATION AND STATISTICAL ANALYSIS

Data treatment and statistical analysis

Data visualization and statistical analysis were performed with OriginPro (OriginLab). In box plots and bar graphs, each data point represents one cell. Box plots show the distribution of data points, the box extends from the 25th to the 75th percentile. The whiskers represent 1 standard deviation (1 SD), the line inside the box shows the median, and the black square is the mean. In bar graphs, the bar represents the mean and the error bars are 1 SD. In the dot-line graphs, the dots represent the mean, and the whiskers show the standard error mean (SEM). Migration data is not normally distributed (tested with the Shapiro-Wilk test). Non-parametric Mann-Whitney U-test was used to test for statistical differences between data sets ($*p < 0.05$, $**p < 0.01$, $***p < 0.001$, $****p < 0.0001$).